

Large-scale anisotropy of Galactic cosmic rays as a probe of local cosmic-ray propagation

AI-FENG LI,¹ QIANG YUAN,^{2,3} WEI LIU,⁴ AND YI-QING GUO^{4,5}

¹*college of Information Science and Engineering, Shandong Agricultural University, Taian 271018, China*

²*Key Laboratory of Dark Matter and Space Astronomy, Purple Mountain Observatory, Chinese Academy of Sciences, Nanjing 210008, China*

³*School of Astronomy and Space Science, University of Science and Technology of China, Hefei 230026, China*

⁴*Key Laboratory of Particle Astrophysics, Institute of High Energy Physics, Chinese Academy of Sciences, Beijing 100049, China*

⁵*University of Chinese Academy of Sciences, Beijing 100049, China*

ABSTRACT

Recent studies have shown that the anisotropy is of great value to decipher cosmic rays' origin and propagation. We have built an unified scenario to describe the observations of the energy spectra and the large-scale anisotropy and called attention to their synchronously evolution with energy. In this work, the impact of the local regular magnetic field (LRMF) and corresponding anisotropic diffusion on large-scale anisotropy have been investigated. When the perpendicular diffusion coefficient is much smaller than the parallel one, the dipole anisotropy points to the LRMF and the observational phase below 100 TeV could be reproduced. Moreover we find that the dipole phase above 100 TeV strongly depends on the evolution of local diffusion. But the current measurements at that energy are still scarce. We suggest that more precise measurements at that energy could be carried out to unveil the local diffusion and further the local turbulence.

1. INTRODUCTION

The understanding of the transport process of cosmic rays (CRs) in Galaxy is crucial to uncover their origin. The past researches are chiefly concerned with the features of energy spectra. Now more and more studies have shown that the CR anisotropy could be another useful observable. Due to the diffusive propagation, the arrival directions of CRs are approximately isotropic in observation. However the mass of evidence has identified that the distribution of the arrival direction is uneven, with the relative intensity varying from $\sim 10^{-4}$ to $\sim 10^{-2}$, which is called anisotropy. So far a lot of experiments have measured the energy dependence of the dipole anisotropy in a wide energy range (Amenomori et al. 2006, 2010, 2017; Guillian et al. 2007; Abdo et al. 2008, 2009; Abbasi et al. 2010, 2011, 2012; Aartsen et al. 2013, 2016; Bartoli et al. 2013, 2015; Abeysekara et al. 2014, 2019). The results show that its evolution with energy is non-trivial. Less than 1 PeV, the dipole amplitude grows up with energy below 10 TeV and above 100 TeV respectively, whereas between 10 TeV and 100 TeV, it indicates a downward trend. What's more, the phase points toward ~ 3 hrs below 100 TeV, which evidently deviates from the Galactic center (which is at about -6 hrs). And above that energy, a flip occurs undoubtedly.

Actually, in the framework of the diffusion model, the uneven distribution of the overall CR sources predicts a large-scale anisotropy. Under the isotropic diffusion, the amplitude of the dipole anisotropy is expected to rise with energy, which soon far exceeds the available measurements, up to two orders of magnitude at ~ 100 TeV, according to the diffusion coefficient inferred from the boron-to-carbon ratio. And the direction of dipole anisotropy aligns with the Galactic center immutably (Blasi & Amato 2012), which goes against with the measurements at low energy. Introducing a local CR source at the direction of anti-Galactic center could partially ease the tension. Since nearby the solar system, the approximation of continuous distribution is no longer valid, the finite and discrete point-like CR sources have to be considered properly. Mertsch (2011) and Bernard et al. (2012) proposed that the finite number of CR sources around the solar system could give rise to the large fluctuations in the observed energy spectrum at high energy, so that the spectral hardening of CR nuclei above 200 GV could originate from the local source. Furthermore when a local CR source is located at the direction of anti-Galactic center, the magnitude of dipole anisotropy could

reduce to the observational level, through cancelling the streaming from the background CR sources (Liu et al. 2017). However, since the contribution from the local source drops off sharply at ~ 100 TeV, the magnitude raises again and outruns observations. Meanwhile the problem of the phase flip is still unsolved.

Another solution for this issue is to modified the diffusion coefficient, i.e. the so-called spatial-dependent propagation (SDP). It was initially proposed to explain the spectral hardening of CR nuclei above 200 GV (Tomassetti 2012; Guo et al. 2016; Liu et al. 2018). Compared with the conventional diffusion model, the diffusion process nearby the Galactic disk is supposed to be much slower. Thereupon the dipole anisotropy could reduce visibly to the observational level. But since the anisotropy is caused by the large-scale distribution of CR sources, the phase points to the Galactic center as well. In the recent works, we established an unified picture to describe energy spectra and anisotropy (Liu et al. 2019; Qiao et al. 2019) by introducing a local source in the SDP model. We proposed that the spectral features and dipole anisotropy have a common origin and they synchronously evolve with energy. The excess of nuclei between 200 GeV and ~ 20 TeV and the anisotropy below 100 TeV are dominated by a local source. Beyond 100 TeV, the background sources override in both energy spectra and dipole anisotropy. The phase at lower energy indicates that the position of local source is close to the direction of anti-Galactic center and far from the Galactic disk. We suggest that the Geminga SNR at its pulsar’s birth place could be a plausible candidate (Zhao et al. 2022). Similar scenarios have also been offered by Fornieri et al. (2021) and Zhang et al. (2022) recently.

In the past years, the study of the emission of energetic neutral atoms by the IBEX experiment revealed that there is a local regular magnetic field within 0.1 pc around the solar system, with the direction at $l \sim 210.5^\circ$ and $b \simeq -57.1^\circ$. The direction of LRMF is coincident with the dipole phase below 100 TeV. The studies of Schwadron et al. (2014), Ahlers (2016) and Liu et al. (2020) demonstrated that this originates from the anisotropic diffusion which guides the CRs propagate along the LRMF. In this work, we focus on the influence of the LRMF and the corresponding anisotropic diffusion on the dipole anisotropy. At lower energy, when the perpendicular diffusion is much smaller, the CRs principally propagate along the LRMF. The dipole phase directs to the LRMF, which well conforms with the measurements. But above 100 TeV, the phase is found to be dependent on the energy dependence of the perpendicular diffusion. If the perpendicular diffusion is still smaller than parallel, the diffusion of CRs is anisotropic and the dipole phase just flips 180° . But if the perpendicular diffusion grows faster and is comparable to the parallel above ~ 100 TeV, the diffusion turns to be isotropic, and the phase directs to the Galactic center. Thereupon, we demonstrate that the dipole phase could be applied to ascertain the local diffusion. However current observations beyond tens of TeV are still lack and the available data have large uncertainties. The precise measurements by e.g. LHAASO, HAWC and ICECUBE experiments, could help determine the evolution of local diffusion with energy and further enhance our understanding of the local turbulence.

2. MODEL DESCRIPTION

2.1. Spatially-dependent propagation

In recent years, the spatial-dependent propagation (SDP) model has been given more and more attention. It was initially introduced as a Two Halo model (Tomassetti 2012) to explain the excess of primary proton and helium fluxes above 200 GeV. Later, it was further used to account for the excess of secondary and heavier components (Tomassetti 2015; Feng et al. 2016; Guo et al. 2016; Liu et al. 2018; Tian et al. 2020; Yuan et al. 2020), diffuse gamma-ray distribution (Guo & Yuan 2018) and large-scale anisotropy (Liu et al. 2019; Qiao et al. 2019; Zhao et al. 2022). The recent measurement of TeV halo around the pulsars found that the CRs diffuse significantly slower than the inference from the boron-to-carbon ratio, which strongly support the assumption that diffusion could be spatial-dependent (Abeysekara et al. 2017; Aharonian et al. 2021).

In the SDP model, the whole diffusive halo is divided into two regions. Nearby the Galactic disk and its surrounding area are called the inner halo (IH) region, the turbulence level is affected by the activities of supernova explosions immensely. Hence it is expected to be intense near the large population of sources and correspondingly the diffusion process is slower, while at regions with fewer sources, the turbulence is moderate and the diffusion tends to be fast. Thus, the diffusion coefficient in the inner halo is relevant to the radial distribution of CR sources. Far away from the Galactic disk, i.e. so-called outer halo (OH) region, the turbulence is less impacted by the stellar activities and believed to be self-generated by CRs themselves, so the diffusion approaches to be only rigidity-dependent.

In this work, the half thickness of the whole diffusive halo is defined as z_h , and IH and OH regions are ξz_h and $(1 - \xi)z_h$ respectively. Both z_h and ξ are determined by fitting B/C ratio and nuclei spectra. The diffusion coefficient

D_{xx} is parameterized as:

$$D_{xx}(r, z, \mathcal{R}) = D_0 F(r, z) \beta^\eta \left(\frac{\mathcal{R}}{\mathcal{R}_0} \right)^{\delta_0 F(r, z)}, \quad (1)$$

in which the reference rigidity \mathcal{R}_0 is fixed to 4 GV. The spatial dependence $F(r, z)$ is written as

$$F(r, z) = \begin{cases} g(r, z) + [1 - g(r, z)] \left(\frac{z}{\xi z_0} \right)^n, & |z| \leq \xi z_h \\ 1, & |z| > \xi z_h \end{cases}. \quad (2)$$

$g(r, z) = N_m/[1 + f(r, z)]$, with $f(r, z)$ representing the spatial distribution of CR sources. The CR sources are approximated as axisymmetric-distributed, i.e. $f(r, z) \propto (r/r_\odot)^\alpha \exp[-\beta(r - r_\odot)/r_\odot] \exp(-|z|/z_s)$, where $r_\odot = 8.5$ kpc and $z_s = 0.2$ kpc. α and β are taken as 1.69 and 3.33 (Case & Bhattacharya 1996).

The injection spectrum of background sources is assumed to have a form of power-law of rigidity with an exponential cutoff, namely

$$Q(\mathcal{R}) \propto \mathcal{R}^{-\nu} \exp\left(-\frac{\mathcal{R}}{\mathcal{R}_c}\right). \quad (3)$$

The diffusion-reacceleration (DR) model is adopted in the propagation equation and the numerical package, DRAGON, is used to compute the background CR distribution (Evoli et al. 2008).

2.2. Local source

In our previous works (Liu et al. 2019; Qiao et al. 2019; Zhao et al. 2022), the spectral anomaly above 200 GV and dipole anisotropy below 100 TeV are attributed to Geminga SNR, which is the remnant after the explosion of Geminga's progenitor. Its characteristic age is inferred from the spin-down luminosity of Geminga pulsar, which is about $\tau = 3.4 \times 10^5$ years (Manchester et al. 2005). The position is backtracked to $l = 194.3^\circ, b = -13^\circ$, and the distance to the solar system is ~ 330 pc (Faherty et al. 2007). The CR flux from the Geminga SNR can be computed by solving the time-dependent diffusion equation using the Green's function method, assuming an boundary at infinity (Liu et al. 2017, 2019). As for the instantaneous and point-like injection, the spatial distribution is

$$\psi(r, \mathcal{R}, t) = \frac{q_{\text{inj}}(\mathcal{R})}{(\sqrt{2\pi}\sigma)^3} \exp\left(-\frac{(\mathbf{r} - \mathbf{r}')^2}{2\sigma^2}\right), \quad (4)$$

where $\sigma(\mathcal{R}, t) = \sqrt{2D_{xx}(\mathcal{R})t}$ is the effective diffusion length within time t . The injection spectrum $q_{\text{inj}}(\mathcal{R})$ is parameterized as a power-law function of rigidity with an exponential cutoff, i.e. $q_0 \mathcal{R}^{-\alpha} \exp(-\mathcal{R}/\mathcal{R}'_c)$.

2.3. Anisotropic diffusion

The IBEX experiment has detected a regular magnetic field with spatial scale ~ 0.1 pc around the solar system (McComas et al. 2009; Funsten et al. 2013). The magnetic field axis is along the direction of $l \simeq 210.5^\circ, b \simeq -57.1^\circ$. Similar finding was reported from the polarization measurements of the local stars (Frisch et al. 2015). This direction is coincident with the dipole phase below 100 TeV (Ahlers 2016). Since that the spatial scale of LRMF is much smaller than the average propagation length inferred from the boron-to-carbon ratio, the LRMF does not have remarkable impact on the energy spectra. But CRs diffuse anisotropically in the local interstellar space under the influence of LRMF and the arrival direction and the corresponding dipole anisotropy is expected to be modified correspondingly. In this case, the diffusion coefficient D is replaced by the tensor D_{ij} , which is written as

$$D_{ij} \equiv D_\perp \delta_{ij} + (D_\parallel - D_\perp) b_i b_j, \quad b_i = \frac{B_i}{|\mathbf{B}|} \quad (5)$$

where b_i is the i -th component of the unit vector of LRMF (Giacalone & Jokipii 1999; Cerri et al. 2017). D_\parallel and D_\perp are the diffusion coefficients parallel and perpendicular to the LRMF, respectively. In this work, each of them is parameterized as a power-law function of rigidity,

$$D_\parallel = D_{0\parallel} \beta^\eta \left(\frac{\mathcal{R}}{\mathcal{R}_0} \right)^{\delta_\parallel}, \quad (6)$$

$$D_\perp = D_{0\perp} \beta^\eta \left(\frac{\mathcal{R}}{\mathcal{R}_0} \right)^{\delta_\perp} = \varepsilon D_{0\parallel} \beta^\eta \left(\frac{\mathcal{R}}{\mathcal{R}_0} \right)^{\delta_\perp}. \quad (7)$$

Tab. 1. Fitted SDP parameters.

D_0	δ_0	N_m	ξ	n	v_A	z_h
$[\text{cm}^2 \cdot \text{s}^{-1}]$					$[\text{km} \cdot \text{s}^{-1}]$	$[\text{kpc}]$
4.87×10^{28}	0.58	0.62	0.1	4	6	5

	Background			Local source		
Element	A^\dagger	ν	\mathcal{R}_c	q_0	α	\mathcal{R}'_c
	$[(\text{m}^2 \cdot \text{sr} \cdot \text{s} \cdot \text{GeV})^{-1}]$		[PV]	$[\text{GeV}^{-1}]$		[TV]
p	1.91×10^{-2}	2.34	7	8.28×10^{52}	2.16	25
He	1.43×10^{-3}	2.27	7	2.35×10^{52}	2.08	25
C	6.15×10^{-5}	2.31	7	7.2×10^{50}	2.13	25
N	7.67×10^{-6}	2.34	7	1.13×10^{50}	2.13	25
O	8.20×10^{-5}	2.36	7	1.11×10^{51}	2.13	25
Ne	8.05×10^{-6}	2.28	7	1.13×10^{50}	2.13	25
Mg	1.62×10^{-5}	2.39	7	1.08×10^{50}	2.13	25
Si	1.28×10^{-5}	2.37	7	1.05×10^{50}	2.13	25
Fe	1.23×10^{-5}	2.29	7	2.20×10^{50}	2.13	25

[†]The normalization is set at total energy $E = 100$ GeV.

Tab. 2. Fitted injection parameters of the background and local sources.

Here $\varepsilon = \frac{D_{0\perp}}{D_{0\parallel}}$ is the ratio between perpendicular and parallel diffusion coefficient at the reference rigidity \mathcal{R}_0 . When taking the local anisotropic diffusion into account, the dipole anisotropy becomes accordingly

$$\delta = \frac{3\mathbf{D} \cdot \nabla\psi}{v\psi} = \frac{3}{v\psi} D_{ij} \frac{\partial\psi}{\partial x_j}. \quad (8)$$

3. RESULTS AND DISCUSSION

First of all, the propagation parameters can be determined by fitting the boron-to-carbon ratio. The LRMF has the spatial scale of ~ 0.1 pc (Funsten et al. 2013), which is much less than the average propagation length of CRs. The propagated energy spectra is hardly impacted by the LRMF. Hence the CR fluxes from both background and local sources could be evaluated in terms of SDP. In the SDP model, the unknown propagation parameters are D_0 , δ_0 , N_m , ξ , n , v_A and z_h , whose values are shown in table 1. In addition, the normalization, power index and cut-off rigidity of background (local) nuclei i in the injection spectra, i.e. A^i , ν^i and \mathcal{R}_c (q_0^i , α^i and \mathcal{R}'_c) have to be settled by fitting the energy spectra. The cutoff rigidities of different compositions are regarded as the limits of acceleration in the sources and assumed to be Z -dependent.

Fig. 1 shows the fitting to the proton (left), helium (right) spectra, in which red, blue and black lines are the contribution from local source, background sources and sum of all respectively. And Fig. 2 illustrates the fitting to the all-particle spectra. The injection parameters of major compositions are listed in table 2. To account for the softening at tens of TeV in proton and helium spectra, the cut-off rigidity of the local source is 25 TV. And to describe the all-particle spectrum as well as cut-offs of proton and helium at PeV energies, the cut-off rigidity of the background sources are 7 PV.

Unlike the energy spectra, the LRMF could dramatically affect the arrival direction of CRs and thus the dipole anisotropy by altering the direction of CR streaming. To study the influence of the LRMF, the anisotropic diffusion in the local environment and thus the anisotropy are investigated. The value measured by the IBEX is chosen as the direction of LRMF. And the parallel diffusion is equal to the diffusion in the SDP. Fig. 3 shows the dipole amplitude and phase by varying ε from 1 to 0.01 with $\delta_\perp = \delta_\parallel$. With ε decreasing, the perpendicular diffusion thus diminishes gradually, which engenders the descent of the overall dipole amplitude. Meanwhile the smaller ε is, the deeper the trench at ~ 100 TeV becomes. This can be understood as follows. The dipole amplitude depends on the CR flow

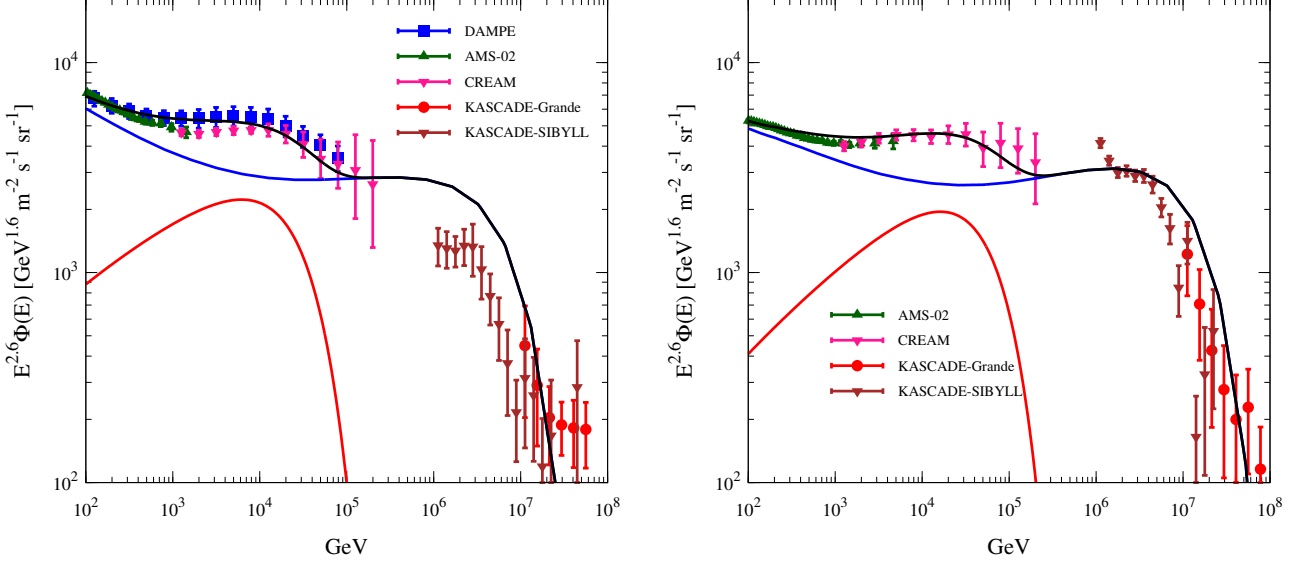


Fig. 1. Energy spectra of protons (left) and helium nuclei (right). The data points are taken from DAMPE(An et al. 2019; Alemanno et al. 2021), AMS-02 (Aguilar et al. 2015, 2017), CREAM-III (Yoon et al. 2017), NUCLEON (Atkin et al. 2017), KASCADE (Antoni et al. 2005) and KASCADE-Grande (Apel et al. 2013) respectively. The blue lines are the background fluxes, and the red lines are the fluxes from a nearby Geminga SNR source respectively. The black lines represent the total fluxes.

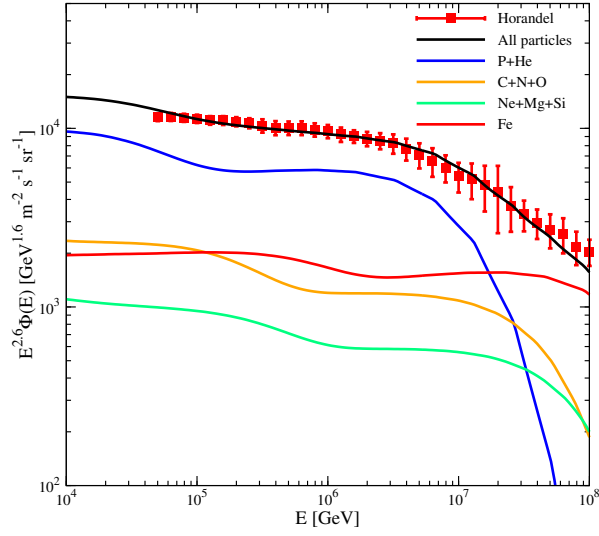


Fig. 2. The all-particle spectra multiplied by $E^{2.6}$. The data points are taken from (Hörandel 2003). The solid lines with different colors are the model predictions of different mass groups, and the black solid line is the total contribution.

$\mathbf{D} \cdot \nabla \psi$. When $\varepsilon \ll 1$, only the CR flow projected along the LRMF play a leading role, while the CR flow perpendicular to the LRMF is suppressed due to the decrease of the perpendicular diffusion. And due to the lack of the CR flow perpendicular to the LRMF, the trench at ~ 100 TeV becomes smaller, namely sharper.

More important, ε also revises the phase, as shown in right of Fig. 3. Less than 100 TeV, the local source, i.e. Geminga SNR, dominates. When ε closes to 1, the diffusion is approximately isotropic and the dipole phase points to the position of Geminga SNR. Above 100 TeV, the background sources dominates and the phase turns to the Galactic center. This corresponds to the regular isotropic diffusion, which is shown as the red line. With the decrease of ε , the dipole phase gradually changes. When ε is less than 0.1, the CR flow tends to propagate along LRMF more, and

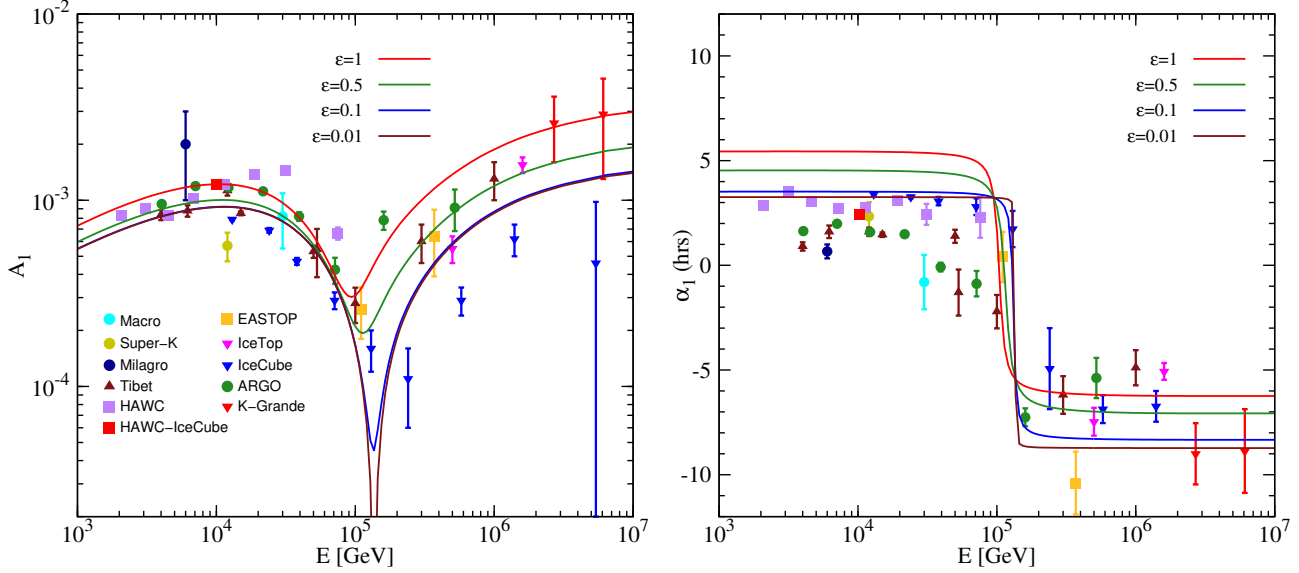


Fig. 3. The energy dependence of the amplitude (left) and phase (right) of the dipole anisotropy when $\epsilon = 1, 0.5, 0.1, 0.01$ respectively with $\delta_{\parallel} = \delta_{\perp}$. The data points are taken from Marco (Ambrosio et al. 2003), SuperKamiokande (Guillian et al. 2007), EAS-TOP (Aglietta et al. 1995, 1996, 2009), Milagro (Abdo et al. 2009), IceCube (Abbasi et al. 2010, 2012), IceTop (Aartsen et al. 2013), ARGO-YBJ (Bartoli et al. 2015), Tibet (Amenomori et al. 2005, 2010, 2017), KASCADE-Grande (Chiavassa et al. 2015), HAWC (Abeysekara et al. 2019), HAWC-IceCube (Abeysekara et al. 2019)

the phase directs to the LRMF less than 100 TeV, which is compatible with the measurements. At higher energy, the background streaming is dominated. The phase makes a 180° flip and points the opposite direction of LRMF, as shown by the blue and brown solid lines. It is worth noting that the transition of dipole phase at ~ 100 TeV also becomes sharper with ϵ decreasing due to lack of the component perpendicular to the LRMF.

Fig. 4 illustrates the influence of δ_{\perp} on dipole anisotropy by defining $\Delta\delta = \delta_{\perp} - \delta_{\parallel}$. Here ϵ is fixed to 0.01 so that the dipole phase orients the LRMF at lower energy. But at higher energy, the dipole anisotropy depends on $\Delta\delta$. When $\Delta\delta$ is close 0, for example 0.1, the perpendicular diffusion grows slower with energy, so that above hundreds of TeV it is still smaller than the parallel one, the phase points to the opposite direction of LRMF, as the red solid shows. But when $\Delta\delta = 0.3$, the perpendicular diffusion grows faster than the parallel and both of them becomes comparable above 100 TeV. In other words, the diffusion converts to be isotropic at that energy. Hence above 100 TeV, the amplitude increases and the orientation changes from LRMF to the Galactic center, see the green line. There is a transition of direction above 100 TeV, from the LRMF to the Galactic center. When the perpendicular diffusion grows much faster than the parallel, for example $\Delta\delta = 0.5$, the diffusion approaches to be isotropic before 100 TeV and the phase changes from the LRMF to the local source. This is disfavored by the available measurements and thus excluded. We conclude that the dipole anisotropy could be applied to constrain the evolution of diffusion process with energy.

In Figure 5, we illustrate the energy dependence of the ratio D_{\perp}/D_{\parallel} by varying $\Delta\delta$ with $\epsilon = 0.01$ (blue) and $\epsilon = 0.001$ (red) respectively. The black solid line corresponds to $\epsilon = 0.1$ and $\delta_{\perp} = \delta_{\parallel}$, i.e. the blue solid line in Figure 3. When the D_{\perp} is always smaller than D_{\parallel} , for example the blue ($\Delta\delta = 0.1, \epsilon = 0.01$) and red ($\Delta\delta = 0.3, \epsilon = 0.001$) dash lines, the dipole phase is always along LRMF, but with a 180° reversal above 100 TeV. When $\Delta\delta = 0.3, \epsilon = 0.01$ and $\Delta\delta = 0.5, \epsilon = 0.001$, i.e. blue and red dash-dot lines, both perpendicular and parallel diffusion are of comparable above 100 TeV, the phase changes gradually from LRMF to the Galactic center. When $\Delta\delta$ is too large, for example 0.5 when $\epsilon = 0.01$ and 0.8 when $\epsilon = 0.001$, the diffusion approaches the isotropic below 100 TeV, the phase points from the LRMF to the local source less than 100 TeV, and turn to the Galactic center at higher energy. Thus the precise measurements of the dipole anisotropy constrain the available range of δ_{\perp} when fixing ϵ . The smaller ϵ is, the larger the available range of δ_{\perp} becomes.

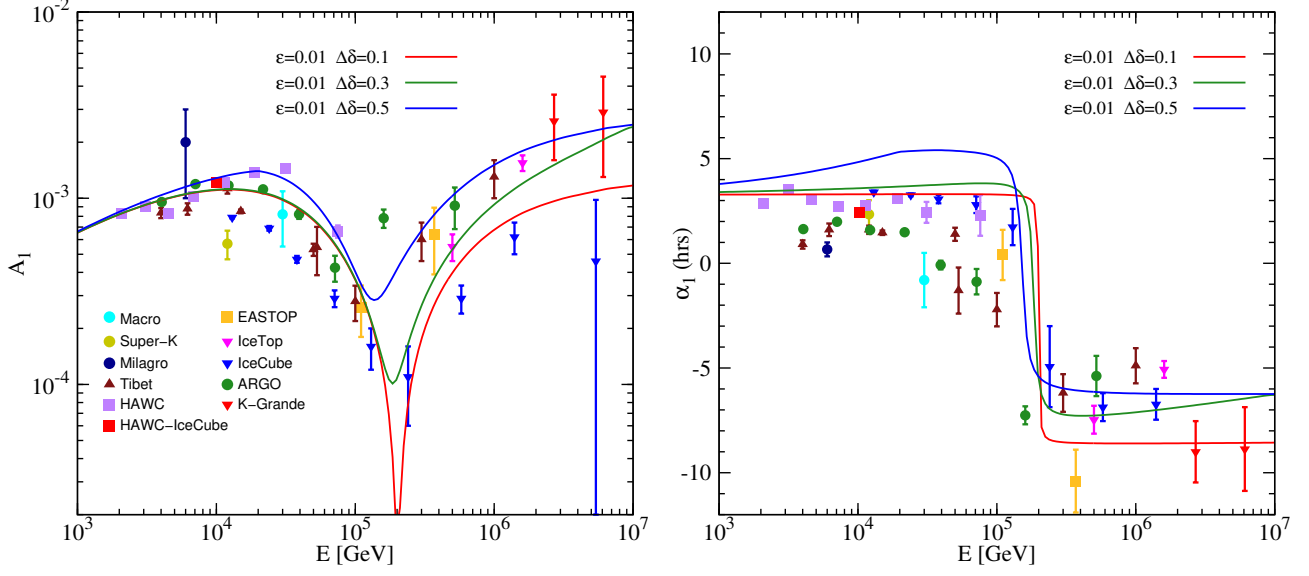


Fig. 4. Energy dependences of the amplitude (left) and phase (right) of the anisotropies for $\varepsilon = 0.01$. The three black lines correspond to $\Delta\delta = \delta_{\perp} - \delta_{\parallel} = 0.1, 0.3, 0.5$ respectively.

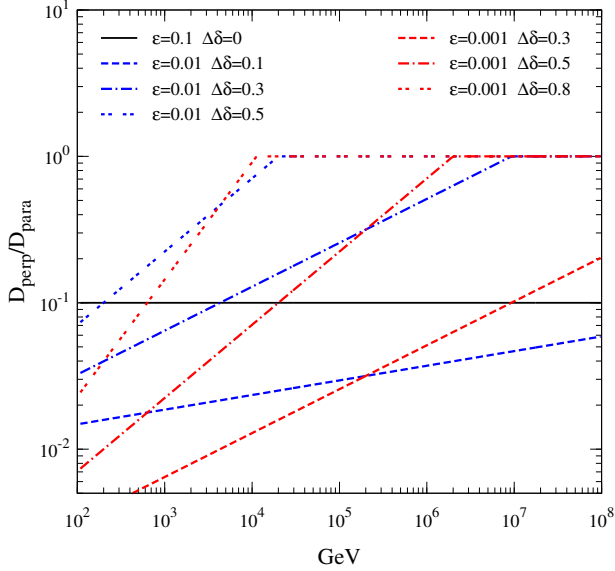


Fig. 5. Energy dependences of D_{\perp}/D_{\parallel} . The black line is the result for $\varepsilon = 0.01$ and $\Delta\delta = 0$. The three blue broken lines correspond to $\Delta\delta = 0.1, 0.3, 0.5$ with $\varepsilon = 0.01$. The three red broken lines correspond to $\Delta\delta = 0.3, 0.5, 0.8$ with $\varepsilon = 0.001$.

However the observations of the anisotropy above 100 TeV are still scarce. The measurements by the AS γ and ICECUBE experiments showed that the phase points to the Galactic center (Aartsen et al. 2016; Amenomori et al. 2017; Bartoli et al. 2018). The KASCADE-Grande's measurement indicated an excess in the anti-LRMF direction at the corresponding energy range (Chiavassa et al. 2015; Ahlers 2016). However, the latest analysis using more KASCADE-Grande data still did not report the dipole anisotropy with high enough significance (Apel et al. 2019; Ahlers 2019). Nevertheless, that the dipole phase above 100 TeV directs to the Galactic center is still not well established, subject to the small data sample and worse energy resolution. Meanwhile due to the limited energy

resolution of ground-base instruments at high energy, the transition of dipole phase above 100 TeV, as the green solid line in Fig. 4 shows, is hard to measure. We hope the precise measurements of the anisotropy with higher energy resolution, for example LHAASO, HAWC and ICECUBE experiments, could untangle that confusion and impose constraints on the energy dependence of parallel and perpendicular diffusion.

4. SUMMARY

The CR anisotropies have been observed for a long time. Recently there is an increasing realization that the large-scale dipole anisotropy could unveil the nearby sources. In the previous works, we built up a self-consistent propagation scenario to explain both the spectral hardening in the energy spectra and the evolution of the dipole anisotropy. In this work, the local regular magnetic field and the corresponding anisotropic diffusion are introduced to study their impact on the dipole anisotropy. The ratio of perpendicular-to-parallel diffusion coefficient at reference rigidity and difference of their power indexes are investigated respectively.

As the perpendicular diffusion diminishes, the CR fluxes are apt to propagate along the LRMF nearby the solar system. Therefore the dipole phase changes from the position of the local source to the direction of the LRMF less than 100 TeV, which is more consistent with the current observations. And above 100 TeV, the phase makes a 180° turnaround and points to the direction of the LRMF. And we notice that the amplitude of anisotropy could reduce due to the decrease of perpendicular diffusion.

However AS γ , ARGO, HAWC and ICECUBE experiments indicate that above 100 TeV, the dipole phase points to the Galactic center. Under the scenario of LRMF, it inevitably hints a transition of diffusion mechanism, in which diffusion turns from anisotropic to isotropic with energy increasing. That means the perpendicular diffusion grows faster than parallel diffusion as energy increases. We study the power index of the perpendicular diffusion compared to the parallel one. The dipole phase between tens of TeV and several PeV could effectively constrain the power index of the perpendicular diffusion for the certain ratio of perpendicular-to-parallel diffusion coefficient at reference rigidity. The measurements of CR anisotropy, for example LHAASO, HAWC and ICECUBE experiments, are expected to help determine the diffusion coefficients and could constrain the local turbulence.

Moreover, we want to call attention that due to the poor knowledge of the detector response, it is hard to directly compare the anisotropy intensities at the various declination bands. That is, the ground-based experiments are incapable of observing CR anisotropies along the Earth's rotation axis. The available observations of anisotropy is still incomplete. The observations just indicate the right ascension below 100 TeV is coincident with the LRMF. To confirm that, a real 2D observation containing declination information is still necessary. To do this, the detector response should be simulated at least to the level $\sim 10^{-3}$. We also hope the space instruments could perform the accurate observations in the near future.

Recently Giacinti & Kirk (2017) investigated the influence of the turbulence on the large-scale anisotropy. They found that the specific turbulence in the local interstellar environment could distort dipole anisotropy by introducing higher order component and reshape the distribution of right ascension. Meanwhile Kuhlén et al. (2022) studied the impact of the specific turbulence on formation of the small-scale anisotropy. In the future work, we would further study how the specific turbulence affects the diffusion and anisotropy.

ACKNOWLEDGEMENTS

This work is supported by the National Key R&D Program of China grant (2018YFA0404202) and the National Natural Science Foundation of China (11963004, 11635011, 11875264, U1831208, U1738205, U2031110) and Shandong Province Natural Science Foundation (ZR2020MA095).

REFERENCES

- | | |
|--|---|
| <p>Aartsen, M. G., Abbasi, R., Abdou, Y., et al. 2013, <i>apj</i>, 765, 55</p> <p>Aartsen, M. G., Abraham, K., Ackermann, M., et al. 2016, <i>apj</i>, 826, 220</p> <p>Abbasi, R., Abdou, Y., Abu-Zayyad, T., et al. 2010, <i>apj</i>, 718, L194</p> <p>—. 2011, <i>apj</i>, 740, 16</p> | <p>—. 2012, <i>apj</i>, 746, 33</p> <p>Abdo, A. A., Allen, B., Aune, T., et al. 2008, <i>Physical Review Letters</i>, 101, 221101</p> <p>Abdo, A. A., Allen, B. T., Aune, T., et al. 2009, <i>apj</i>, 698, 2121</p> <p>Abeysekara, A. U., Alfaro, R., Alvarez, C., et al. 2014, <i>apj</i>, 796, 108</p> |
|--|---|

- Abeysekara, A. U., Albert, A., Alfaro, R., et al. 2017, *Science*, 358, 911
- Abeysekara, A. U., Alfaro, R., Alvarez, C., et al. 2019, *ApJ*, 871, 96
- Aglietta, M., Alessandro, B., Antonioli, P., et al. 1995, in *International Cosmic Ray Conference*, Vol. 2, *International Cosmic Ray Conference*, 800
- Aglietta, M., Alessandro, B., Antonioli, P., et al. 1996, *ApJ*, 470, 501
- Aglietta, M., Alekseenko, V. V., Alessandro, B., et al. 2009, *ApJ*, 692, L130
- Aguilar, M., Aisa, D., Alpat, B., et al. 2015, *Phys. Rev. Lett.*, 114, 171103
- Aguilar, M., Ali Cavazonza, L., Alpat, B., et al. 2017, *Phys. Rev. Lett.*, 119, 251101
- Aharonian, F., An, Q., Axikegu, Bai, L. X., et al. 2021, *Phys. Rev. Lett.*, 126, 241103
- Ahlers, M. 2016, *Physical Review Letters*, 117, 151103
- . 2019, *ApJ*, 886, L18
- Alemanno, F., An, Q., Azzarello, P., et al. 2021, *Phys. Rev. Lett.*, 126, 201102
- Ambrosio, M., Antolini, R., Baldini, A., et al. 2003, *Phys. Rev. D*, 67, 042002
- Amenomori, M., Ayabe, S., Cui, S. W., et al. 2005, *ApJ*, 626, L29
- Amenomori, M., Ayabe, S., Bi, X. J., et al. 2006, *Science*, 314, 439
- Amenomori, M., Bi, X. J., Chen, D., et al. 2010, *ApJ*, 711, 119
- . 2017, *ApJ*, 836, 153
- An, Q., Asfandiyarov, R., Azzarello, P., et al. 2019, *Science Advances*, 5, eaax3793
- Antoni, T., Apel, W. D., Badea, A. F., et al. 2005, *Astroparticle Physics*, 24, 1
- Apel, W. D., Arteaga-Velázquez, J. C., Bekk, K., et al. 2013, *Astroparticle Physics*, 47, 54
- . 2019, *ApJ*, 870, 91
- Atkin, E., Bulatov, V., Dorokhov, V., et al. 2017, *J. Cosmology Astropart. Phys.*, 2017, 020
- Bartoli, B., Bernardini, P., Bi, X. J., et al. 2013, *prd*, 88, 082001
- . 2015, *apj*, 809, 90
- . 2018, *ApJ*, 861, 93
- Bernard, G., Delahaye, T., Salati, P., & Taillet, R. 2012, *Astronomy and Astrophysics*, 544, A92
- Blasi, P., & Amato, E. 2012, *jcap*, 1, 11
- Case, G., & Bhattacharya, D. 1996, *A&AS*, 120, 437
- Cerri, S. S., Gaggero, D., Vittino, A., Evoli, C., & Grasso, D. 2017, *jcap*, 10, 019
- Chiavassa, A., Apel, W. D., Arteaga-Velázquez, J. C., et al. 2015, in *International Cosmic Ray Conference*, Vol. 34, *34th International Cosmic Ray Conference (ICRC2015)*, 281
- Evoli, C., Gaggero, D., Grasso, D., & Maccione, L. 2008, *Journal of Cosmology and Astroparticle Physics*, 2008, 018
- Faherty, J., Walter, F. M., & Anderson, J. 2007, *Ap&SS*, 308, 225
- Feng, J., Tomassetti, N., & Oliva, A. 2016, *Phys. Rev. D*, 94, 123007
- Fornieri, O., Gaggero, D., Guberman, D., et al. 2021, *Phys. Rev. D*, 104, 103013
- Frisch, P. C., Berdyugin, A., Piirola, V., et al. 2015, *ApJ*, 814, 112
- Funsten, H. O., DeMajistre, R., Frisch, P. C., et al. 2013, *ApJ*, 776, 30
- Giacalone, J., & Jokipii, J. R. 1999, *ApJ*, 520, 204
- Giacinti, G., & Kirk, J. G. 2017, *ApJ*, 835, 258
- Guillian, G., Hosaka, J., Ishihara, K., et al. 2007, *Phys. Rev. D*, 75, 062003
- Guo, Y.-Q., Tian, Z., & Jin, C. 2016, *ApJ*, 819, 54
- Guo, Y.-Q., & Yuan, Q. 2018, *Phys. Rev. D*, 97, 063008
- Hörandel, J. R. 2003, *Astroparticle Physics*, 19, 193
- Kuhlen, M., Phan, V. H. M., & Mertsch, P. 2022, *ApJ*, 927, 110
- Liu, W., Bi, X.-J., Lin, S.-J., Wang, B.-B., & Yin, P.-F. 2017, *prd*, 96, 023006
- Liu, W., Guo, Y.-Q., & Yuan, Q. 2019, *jcap*, 2019, 010
- Liu, W., Lin, S.-j., Hu, H.-b., Guo, Y.-q., & Li, A.-f. 2020, *ApJ*, 892, 6
- Liu, W., Yao, Y.-h., & Guo, Y.-Q. 2018, *ApJ*, 869, 176
- Manchester, R. N., Hobbs, G. B., Teoh, A., & Hobbs, M. 2005, *AJ*, 129, 1993
- McComas, D. J., Allegrini, F., Bochsler, P., et al. 2009, *Science*, 326, 959
- Mertsch, P. 2011, *Journal of Cosmology and Astroparticle Physics*, 2011, 031
- Qiao, B.-Q., Liu, W., Guo, Y.-Q., & Yuan, Q. 2019, *jcap*, 2019, 007
- Schwadron, N. A., Adams, F. C., Christian, E. R., et al. 2014, *Science*, 343, 988
- Tian, Z., Liu, W., Yang, B., et al. 2020, *Chinese Physics C*, 44, 085102
- Tomassetti, N. 2012, *apj*, 752, L13
- . 2015, *Phys. Rev. D*, 92, 081301
- Yoon, Y. S., Anderson, T., Barrau, A., et al. 2017, *ApJ*, 839, 5
- Yuan, Q., Qiao, B.-Q., Guo, Y.-Q., Fan, Y.-Z., & Bi, X.-J. 2020, *Frontiers of Physics*, 16, 24501

Zhang, Y., Liu, S., & Zeng, H. 2022, MNRAS, 511, 6218

Zhao, B., Liu, W., Yuan, Q., et al. 2022, ApJ, 926, 41